High-resolution solid-state NMR of anisotropically mobile molecules under very low-power ^{1}H decoupling and moderate magic-angle spinning

Tim Doherty, Mei Hong *

Department of Chemistry, Iowa State University, Gilman 0108, Ames, IA 50011, USA

ABSTRACT

We show that for observing high-resolution heteronuclear NMR spectra of anisotropically mobile systems with order parameters less than 0.25, moderate magic-angle spinning (MAS) rates of ~11 kHz combined with ^{1}H decoupling at 1–2 kHz are sufficient. Broadband decoupling at this low ^{1}H nutation frequency is achieved by composite pulse sequences such as WALTZ-16. We demonstrate this moderate MAS low-power decoupling technique on hydrated POPC lipid membranes, and show that 1 kHz ^{1}H decoupling yields spectra with the same resolution and sensitivity as spectra measured under 50 kHz ^{1}H decoupling when the same acquisition times (~50 ms) are used, but the low-power decoupled spectra give higher resolution and sensitivity when longer acquisition times (>150 ms) are used, which are not possible with high-power decoupling. The limits of validity of this approach are explored for a range of spinning rates and molecular mobilities using more rigid membrane systems such as POPC/cholesterol mixed bilayers. Finally, we show ^{15}N and ^{13}C spectra of a uniaxially diffusing membrane peptide assembly, the influenza A M2 transmembrane domain, under 11 kHz MAS and 2 kHz ^{1}H decoupling. The peptide ^{15}N and ^{13}C intensities at low-power decoupling are 70–80% of the high-power decoupled intensities. Therefore, it is possible to study anisotropically mobile lipids and membrane peptides using liquid-state NMR equipment, relatively large rotors, and moderate MAS frequencies.

© 2009 Elsevier Inc. All rights reserved.

1. Introduction

Very fast magic-angle spinning (MAS) frequencies of greater than 40 kHz combined with low-field ^{1}H decoupling of 5–25 kHz has been shown to yield heteronuclear spectra of rigid organic solids with comparable linewidths and sensitivities to those measured under high-power ^{1}H decoupling [1–5]. The primary motivation for low-power ^{1}H decoupling is to allow fast MAS frequencies to be used on high-field NMR spectrometers, so that the increased chemical shift anisotropy (CSA) sidebands can be removed without a concomitant increase in the ^{1}H decoupling field strength or the recoupling of the heteronuclear dipolar interaction by the rotary resonance phenomenon [6]. Low-power decoupling also reduces the radio frequency (rf) load on the spectrometer and allows shorter recycle delays to be used, thus increasing the sensitivity per unit time. This fast MAS – low-power decoupling approach has been demonstrated on small amino acids and large microcrystalline proteins [1,3], all of which are rigid solids. However, a necessary cost of spinning at 40 kHz or higher is that very small rotors (<2 mm outer diameter) with sample volumes of less than 5 μL must be used. This severely restricts the range of systems that can be investigated with this approach. In particular, mem-

brane-bound peptides and proteins that are already diluted by the lipids cannot be easily studied in such small sample volumes.

Since the criterion for fast MAS is that the spinning rate is larger than the strength of the heteronuclear dipolar interaction to be suppressed, mobile semi-solids such as lipid bilayers and peptides embedded in them should benefit from low-power decoupling at much lower MAS frequencies and rf irradiation fields than required for rigid solids. The fact that hydrated lipid membranes are also more susceptible to rf-induced sample heating and degradation gives further incentive to explore the regime of low-power decoupling and fast MAS for hydrated biological membrane samples [7].

MAS frequencies of 10–15 kHz have been used before for ^{1}H NMR of lipids [8] and mobile proteins [9,10] in lipid membranes. The narrowing of ^{1}H lines under these MAS frequencies in the absence of homonuclear decoupling allows high-resolution ^{1}H–^{13}C or ^{1}H–^{15}N heteronuclear correlation spectra to be measured with ^{1}H detection, as shown for cholesterol in deuterated DMPC bilayers [11], or with ^{15}N detection, as shown for a membrane peptide in deuterated DMPC lipids [12]. However, to our knowledge, moderately fast MAS frequencies have not been combined with low-power ^{1}H decoupling to obtain high-resolution heteronuclear spectra. Here we show that for anisotropically mobile lipids and membrane peptides with segmental order parameters of 0.25 and smaller, moderate MAS speeds achievable on 4 mm o.d. rotors (11–15 kHz) and very low ^{1}H decoupling fields of 1–2 kHz are suf-

* Corresponding author. Fax: +1 515 294 0105.
E-mail address: mhong@iastate.edu (M. Hong).

ficient to give similar spectral resolution and intensity as spectra measured under high decoupling fields. In practice, low-power ^{1}H decoupling yields higher resolution than high-power decoupling for hydrated lipids, due to the fact that longer acquisition times can be used without undesirable rf heating and sample degradation. The ability to measure high-resolution heteronuclear spectra of membrane systems using moderately fast MAS frequencies and low-power ^{1}H decoupling allows dilute isotopically labeled membrane peptides to be studied without severe volume limitations, thus enhancing sensitivity.

2. Materials and methods

2.1. Membrane samples

All lipids were obtained from Avanti Polar Lipids (Alabaster, AL) and used without further purification. POPC and POPC/cholesterol (3:2) membranes were prepared by dissolving the lipids in chloroform, drying them under nitrogen gas to remove the solvent, then dissolving the lipid film in cyclohexane and lyophilizing overnight. The dry and homogeneous lipid powder was suspended in water, subject to freeze-thawing five times, then centrifuged at 150,000g for 3 h to produce a membrane pellet. The pellet was lyophilized, packed into 4 mm rotors, then rehydrated to 35 wt.% water. This procedure gives a low-salt membrane sample with a well defined hydration level.

In addition to lipids, the transmembrane peptide of the influenza A M2 protein (M2TMP), which forms a pH-gated proton channel [13], was used to demonstrate the validity of this moderate MAS – low-power decoupling method on mobile membrane peptides [14]. The peptide contains uniformly ^{13}C, ^{15}N-labeled residues at V28, S31 and L36, and was reconstituted into DLPC bilayers by detergent dialysis as described previously [15]. The membrane peptide sample was prepared at pH 7.5, which corresponds to the closed state of the proton channel. The sample also contains amantadine, which gives higher resolution spectra than the apo peptide [16].

2.2. Solid-state NMR experiments

MAS experiments were carried out on a Bruker DSX-400 spectrometer (Karlsruhe, Germany) operating at Larmor frequencies of 400.49 MHz for ^{1}H, 100.70 MHz for ^{13}C, and 40.58 MHz for ^{15}N. A MAS probe equipped with a 4 mm spinner was used for all experiments. ^{1}H–^{13}C and ^{1}H–^{15}N cross-polarization (CP) for the peptide-containing sample was carried out at a spin-lock field strength of 50 kHz for 0.5–1.0 ms. ^{13}C chemical shifts were externally referenced to the α-Glycine ^{13}C CO resonance at 176.49 ppm on the TMS scale and ^{15}N chemical shifts were externally referenced to the ^{15}N resonance of N-acetylvaline at 122 ppm on the NH$_3$ scale.

Low-power decoupled spectra used the WALTZ-16 composite pulse sequence [17] to achieve broadband decoupling. The ^{1}H nutation frequencies ranged from 1 kHz to 11 kHz, and were measured by direct observation of the ^{1}H spectra of lipids. High-power decoupled spectra used TPPM decoupling [18] with a field strength of 50 kHz for the lipid samples and 63 kHz for the peptide-containing sample.

Most ^{13}C direct-polarization spectra of lipid-only samples used acquisition times of 51 ms with 4096 data points. The time-domain data were zero filled to 16,384 points and Fourier-transformed with 3 Hz Lorentzian broadening except when indicated otherwise. Longer acquisition times were not used in comparisons of high-power and low-powder decoupled spectra, since high-power decoupling for more than 50 ms is deemed detrimental to the

probe and sample. To determine the ultimate resolution and sensitivity of the lipid membranes under 11 kHz MAS, we measured a 1 kHz ^{1}H decoupled ^{13}C spectrum of POPC lipids with an acquisition time of 150 ms. For the peptide-containing sample, the ^{13}C CP spectra were measured with an acquisition time of 25.7 ms and processed with 35 Hz Gaussian line broadening, and the ^{15}N CP spectra were measured with an acquisition time of 17.6 ms with 70 Hz Gaussian line broadening.

3. Results and discussion

3.1. Theory for low-power decoupling and moderately fast MAS of uniaxially diffusive systems

The theory of fast MAS and low-power ^{1}H decoupling has been described in detail by Ernst et al. [1]. Below we briefly summarize this theory and point out the differences between uniaxially mobile systems and rigid solids. Under fast MAS and low-power decoupling, we consider the nuclear spin interactions to be averaged first by MAS and then by rf irradiation. For SI_N spin systems under infinite speed MAS, the average Hamiltonian collapses to the zero-order terms, which contain only interactions expected for an isotropic solution, namely isotropic chemical shifts (H^{iCS}) of the I and S spins, and the homonuclear (H_{II}^J) and heteronuclear (H_{SI}^J) J couplings:

$$\bar{H}_{\omega_r \to \infty}^{(0)} = \frac{1}{\tau_r} \int_0^{\tau_r} dt \cdot H(t) = H_S^{iCS} + H_I^{iCS} + H_{II}^J + H_{SI}^J \tag{1}$$

Under finite MAS frequencies, we need to consider the first-order terms in the average Hamiltonian. Higher than first-order terms scale with the MAS frequency as $(1/\omega_r)^2$ and higher powers, thus are not considered here. The first-order terms result from time-dependent commutators between the various interactions:

$$\bar{H}^{(1)} = \frac{-i}{2\tau_r} \int_0^{\tau_r} dt_2 \int_0^{t_2} dt_1 \cdot [H(t_2), H(t_1)]. \tag{2}$$

In general, there are three non-vanishing cross-terms from the above commutator. They are the cross-term between the I–I homonuclear dipolar coupling and the I–S heteronuclear dipolar coupling:

$$\bar{H}_{II,IS}^{(1)} = \frac{1}{\omega_r} \sum_{k \neq l} \overline{\omega}_{skl} S_z I_{kx} I_{ly}, \tag{3}$$

the cross-term between the I–I homonuclear dipolar coupling and I-spin CSA:

$$\bar{H}_{II,I}^{(1)} = \frac{1}{\omega_r} \sum_{k \neq l} \overline{\omega}_{kl} I_{kx} I_{ly}, \tag{4}$$

and the cross-term of the I–I homonuclear dipolar coupling with itself:

$$\bar{H}_{II,II}^{(1)} = \frac{1}{\omega_r} \sum_{i \neq k \neq l} \overline{\omega}_{ikl} I_{iz} I_{kx} I_{ly}. \tag{5}$$

In these expressions, the coupling cross-terms $\overline{\omega}$ have the unit of frequency squared $(rad/s)^2$ due to the commutation.

For uniaxially diffusive lipids and peptides in biological membranes, the I–I homonuclear coupling cross-term (Eq. (5)) vanishes because all motionally averaged dipolar couplings within each lipid and between adjacent lipid molecules are parallel to the motional axis, the bilayer normal, thus they have the same orientation dependence. Analytically, the homonuclear dipolar coupling between spin i and k can be written as $\omega_{ik}(t) = \bar{\delta}_{ik} \cdot \omega(\beta, \gamma, t)$, where β and γ are the polar coordinates of the local bilayer normal with respect to the rotor axis and are the same for all spin pairs, and $\bar{\delta}_{ik}$ is the motionally averaged coupling constant.

As a result, the self-commutation of the homonuclear dipolar coupling becomes:

$$[H_{II}(t_2), H_{II}(t_1)]$$

$$= \left[\sum_{i \neq k} \overline{\delta}_{ik} \cdot \omega(\beta, \gamma, t_2) \left(3I_z^i I_z^k - I^i \cdot I^k \right), \sum_{i \neq k} \overline{\delta}_{ik} \cdot \omega(\beta, \gamma, t_1) \left(3I_z^i I_z^k - I^i \cdot I^k \right) \right]$$

$$= \omega(\beta, \gamma, t_2) \omega(\beta, \gamma, t_1) \left[\sum_{i \neq k} \overline{\delta}_{ik} \left(3I_z^i I_z^k - I^i \cdot I^k \right) \sum_{i \neq k} \overline{\delta}_{ik} \left(3I_z^i I_z^k - I^i \cdot I^k \right) \right] = 0.$$

(6)

The I-spin CSA and I–I dipolar cross-term in Eq. (4) does not directly lead to S spectral broadening since it only involves the I spins. But the I–I and I–S dipolar cross-term in Eq. (3) leads to S broadening through the heteronuclear dipolar coupling. To obtain narrow S spectra, one needs to decouple at a ω_1 nutation frequency either much higher than ω_r or much lower than ω_r but still adequate to remove the remaining S–I dipolar interaction. In the latter regime $\omega_1 << \omega_r$, the rotary resonance recoupling condition $\omega_1 = n\omega_r (n = 1, 2)$ does not apply, thus no line broadening from rotary resonance will occur.

Under the condition that the decoupling field is lower than the spinning rate but higher than the MAS-averaged spin interactions in Eqs. (3) and (4), transformation to an interaction frame defined by the rf field and a second averaging leads to the zero-order average Hamiltonian:

$$\overline{\overline{H}}^{(0)} = H_S^{iCS} + H_{II}^J.$$

(7)

Compared to the rigid solid case, no homonuclear dipolar coupling term remains for the uniaxially mobile system [1]. Comparing Eqs. (1), (3), and (7), it can be seen that low-power decoupling removes the I–S J-coupling and suppresses the cross-term between the homonuclear and heteronuclear dipolar coupling.

For rigid solids, MAS rates $\omega_r/2\pi$ larger than 40 kHz and rf fields $\omega_1/2\pi$ smaller than ~20 kHz were found to be the fast spinning and low-power decoupling regimes, respectively. We can estimate the prefactor $\overline{\omega}_{skl}/\omega_r$ in Eq. (3) as follows. Using the one-bond C–H dipolar coupling of 22 kHz and the geminal H–H dipolar coupling of 25 kHz, and assuming an MAS rate of 50 kHz, a CH$_2$ spin system has a prefactor of:

$$\frac{\overline{\omega}_{skl}}{\omega_r} \propto \frac{\omega_{IS} \cdot \omega_{II}}{\omega_r} \approx \frac{(2\pi \times 22 \text{ kHz}) \times (2\pi \times 25 \text{ kHz})}{2\pi \times 50 \text{ kHz}} \approx 2\pi \times 11 \text{ kHz,}$$

(8)

This prefactor matches well the experimental observation that at 50 kHz MAS, a ^{1}H decoupling field of less than 15 kHz causes broadening of the CH$_2$ signal [2]. For C–H spin systems, the prefactor is smaller, about 2.5 kHz, due to the weaker H–H dipolar coupling. Correspondingly, the measured threshold ^{1}H decoupling field decreases to ~8 kHz, below which line broadening occurs.

For uniaxially mobile lipids where the segmental order parameters S_{CH} are in the range 0.02–0.25 [19], the spinning frequency and decoupling field requirements are correspondingly lower. Assuming an intermediate order parameter of 0.10 for a typical lipid group, the residual heteronuclear dipolar coupling prefactor for a CH$_2$ group under 11 kHz MAS can be estimated as:

$$\frac{\overline{\omega}_{skl}}{\omega_r} \propto \frac{\overline{\omega}_{IS} \cdot \overline{\omega}_{II}}{\omega_r} \approx \frac{(2\pi \times 22 \times 0.1 \text{ kHz}) \times (2\pi \times 25 \times 0.1 \text{ kHz})}{2\pi \times 11 \text{ kHz}} \approx 2\pi \times 0.5 \text{ kHz,}$$

(9)

Thus, a ^{1}H decoupling field of ~1 kHz should be sufficient to suppress this residual coupling. This suggests that moderately fast MAS frequencies that are readily achievable on 4 mm rotors may allow lipid membranes and even membrane peptides to be studied

under extremely low-power ^{1}H decoupling. In this ω_1 regime, composite pulse sequences such as WALTZ-16 [17] are necessary to achieve broadband decoupling.

3.2. Low-power decoupling of low-viscosity hydrated lipid membranes

Fig. 1(a and b) shows the ^{13}C direct polarization (DP) spectra of hydrated POPC membranes under 11 kHz MAS with 1 kHz WALTZ-16 decoupling (a) and 50 kHz TPPM decoupling (b). Both spectra were processed with 3 Hz of Lorentzian broadening to reduce truncation wiggles. It can be seen that the intensities and linewidths of the low-power decoupled spectrum is comparable to or better than the high-power decoupled spectrum. For a clearer view of the intensities and linewidths, Fig. 2 shows expanded regions of the ^{13}C spectra of the lipid chain CH$_2$ resonance at 31 ppm (a) and the glycerol G2 peak at 71 ppm (b) as a function of the ^{1}H decoupling field. These two resonances are chosen because they are the most rigid segments in hydrated phosphocholine, as manifested by their relatively large C–H order parameters [20], and thus are the most difficult sites to decouple well. Fig. 2 shows that both resonances broaden and decrease in intensities with increasing ^{1}H decoupling field $\omega_1/2\pi$, with the minimum intensity at the rotary resonance condition of $\omega_1 = \omega_r$ at 11 kHz. This is expected due to the recoupling of the C–H heteronuclear interaction. For all resonances, the maximum intensity is observed at the lowest decoupling field of 1 kHz.

At the HORROR condition of $\omega_1 = \omega_r/2$, it is known that recoupling of the homonuclear dipolar coupling I–I enhances I-spin spin diffusion and leads to line narrowing of the heteronuclear spectra by self-decoupling [21]. This effect has been observed in rigid ^{13}C-labeled model compounds [2]. We do not observe this HORROR line narrowing effect at $\omega_1/2\pi = 5.5$ kHz for the lipids (Fig. 2). This is consistent with the suppression of the I–I homonuclear dipolar coupling cross-term by uniaxial motion as shown in Eq. (6). In addition, in contrast to rigid solids [2], we do not observe line broadening at low decoupling fields of $\omega_1/\omega_r < 0.25$. Down to 1 kHz decoupling, the intensity increased monotonically. This is again expected from the estimated prefactor for the residual dipolar interactions of lipids (Eq. (9)). When no ^{1}H decoupling is applied, the ^{13}C spectrum of POPC membrane under 11 kHz MAS (Fig. 3) shows ^{13}C–^{1}H J-splittings with linewidths of 10–25 Hz, which are only slightly larger than the linewidths of the best decoupled spectra, which are 7–20 Hz. This means that 11 kHz MAS is already sufficient to suppress most of the residual heteronuclear interactions, and low-power decoupling mainly serves to suppress the ^{13}C–^{1}H scalar coupling in a broadband fashion.

A practical advantage of the very low-power decoupling under moderately fast MAS is that it allows suitably long acquisition times to be used for hydrated membranes. With an acquisition time of 50 ms, the lipid spectra still exhibit truncation wiggles for many peaks such as the highly averaged headgroup Cγ at 54.6 ppm (Fig. 1a and b). When a full acquisition time of 150 ms was used under 1 kHz decoupling, the linewidths of the lipid ^{13}C spectrum are found to be 7–20 Hz (Fig. 1c). This long acquisition time is not possible under high-power decoupling conditions.

3.3. Limits of applicability: spinning speed, temperature, and mobility

To test whether the low-power decoupling and moderately fast MAS approach works for a wide range of membrane systems, we investigated the ^{13}C spectral resolution and intensity as a function of MAS frequency, temperature, and lipid mobility. Fig. 4 shows the glycerol G2 region of the ^{13}C DP spectra of hydrated POPC lipids for a number of MAS frequencies under the same ^{1}H decoupling field of 1 kHz. At 9 kHz spinning the spectrum shows similar intensity to the 11 kHz MAS spectrum, but decreasing the spinning speed
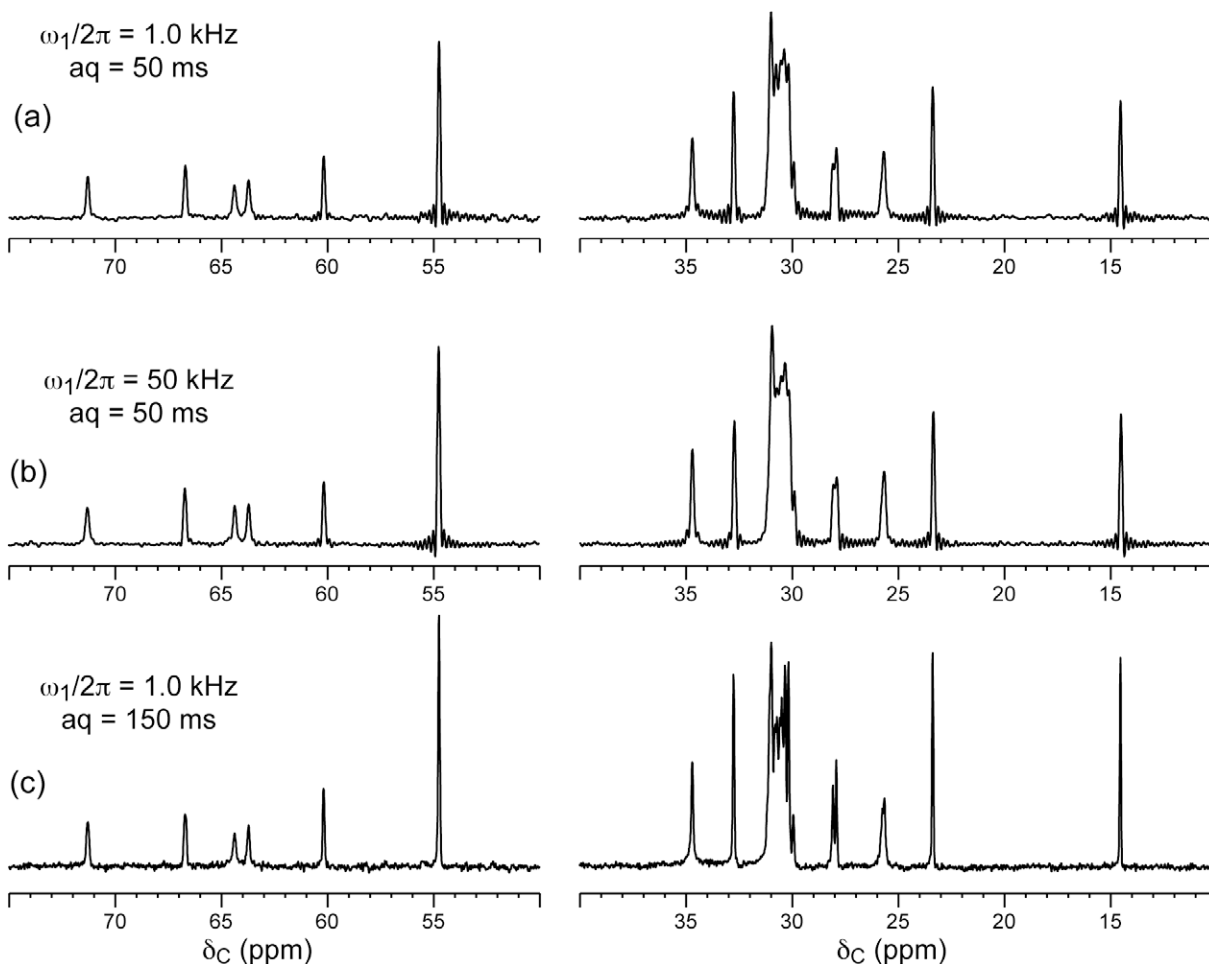
Fig. 1. Direct polarization ^{13}C spectra of hydrated POPC bilayers under 11 kHz MAS at 293 K with different ^{1}H decoupling methods. (a) 1.0 kHz WALTZ-16 decoupling, with a 50 ms acquisition time. (b) 50 kHz TPPM decoupling, with a 50 ms acquisition time. (c) 1.0 kHz WALTZ-16 decoupling with a 150 ms acquisition time. Spectra (a) and (b) were processed with 3 Hz Lorentzian broadening, while spectrum (c) did not use any line broadening.
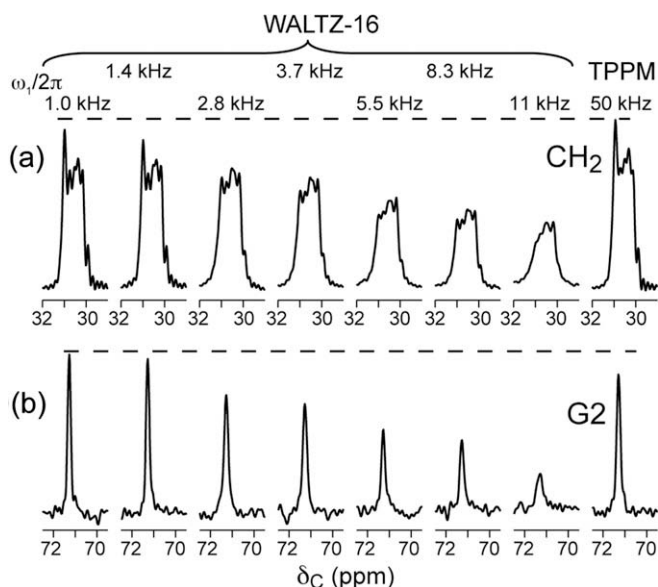

Fig. 2. Expanded regions of the ^{13}C direct-polarization spectra of hydrated POPC lipids. (a) Lipid chain CH$_2$ peaks. (b) Lipid glycerol G2 peak. The ^{1}H decoupling method and field strengths are indicated above the individual spectra. Dashed lines guide the eye for the maximum intensity.

to 7 kHz and below clearly decreases the intensities under low-power decoupling. Thus, for hydrated lipids, the minimum spinning rate necessary to achieve MAS averaging of the dipolar interaction is about 10 kHz.

The next two tests explore the effect of increased molecular rigidity on the low-power decoupling efficiency. When the hydrated POPC membrane is cooled to below its phase transition temperature of 270 K, the ^{13}C DP spectra showed higher intensities and narrower lines under higher power decoupling than low-power decoupling (Fig. 5). Although we did not measure the C–H order parameters of the gel-phase POPC lipids, ^{2}H quadrupolar splittings from the literature suggest that the order parameters increase by a factor of 2 [22].

Cholesterol-containing membranes are of interest both for understanding the fundamental biophysics of domain formation in lipid membranes and for mimicking eukaryotic membranes. Addition of cholesterol to phospholipids is well known to make the lipid membrane less elastic, with order parameters increasing by about a factor of 2 [23]. Fig. 6 shows three representative peaks of POPC and cholesterol in the mixed POPC/cholesterol (3:2) membrane under 11 kHz MAS and various ^{1}H decoupling fields. It can be seen that the moderately fast MAS rate is insufficient to narrow the cholesterol ring ^{13}C peaks due to the rigidity of the sterol rings. However, the resolved aliphatic peaks of cholesterol such as C26 and C27 at 23.1 ppm vary in intensity with decoupling in a similar fashion as the POPC resonances. For the POPC lipids in this mem-
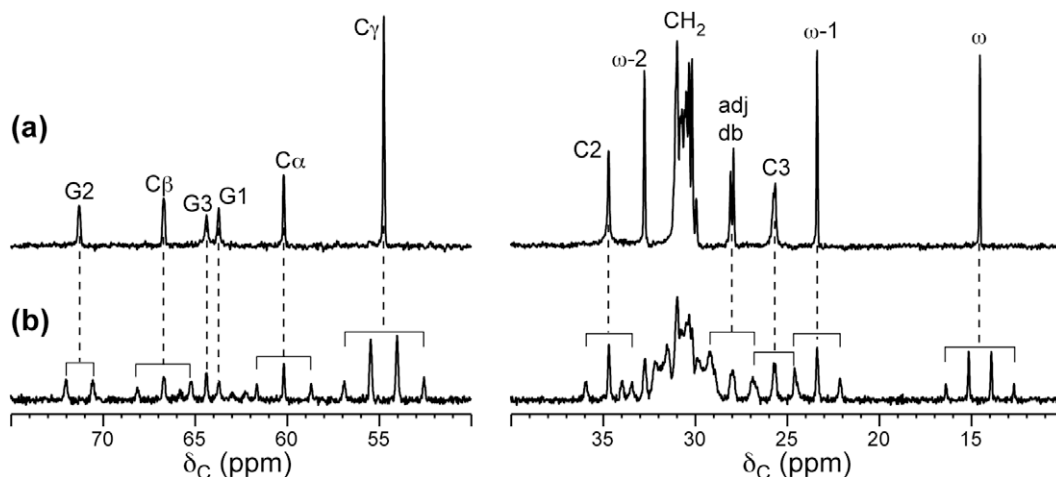
Fig. 3. POPC ¹³C direct-polarization spectra at 293 K under 11 kHz MAS. Both spectra were measured with an acquisition time of 150 ms. (a) WALTZ-16 ¹H decoupled spectrum with $\omega_1/2\pi = 1$ kHz. (b) ¹H undecoupled spectrum. The FWHM linewidths of the peaks are 7–20 Hz in (a) and 10–25 Hz in (b).
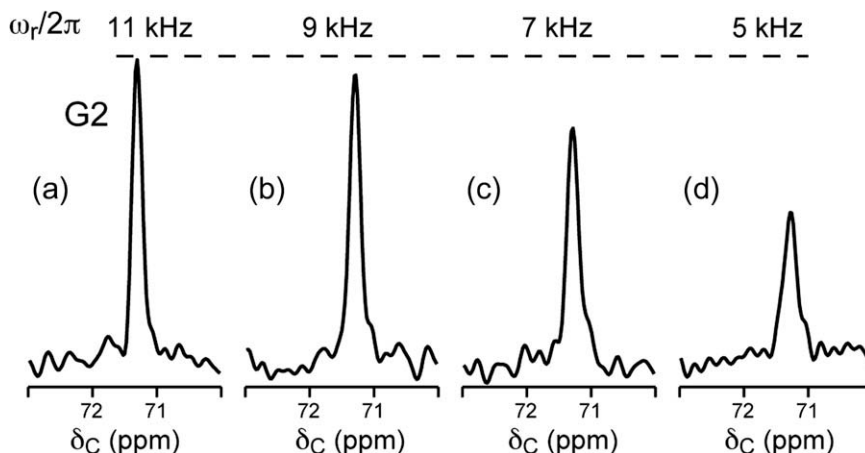

Fig. 4. Low-power decoupled POPC glycerol G2 intensity as a function of MAS frequency at 293 K. All spectra were measured with 1.0 kHz WALTZ-16 ¹H decoupling. Spinning rates are (a) 11 kHz, (b) 9 kHz, (c) 7 kHz, and (d) 5 kHz.

brane mixture, the ¹³C intensities at low-power decoupling are similarly narrow as the pure POPC sample.

3.4. Uniaxially mobile membrane peptides under low-power decoupling and moderate MAS

Since the basic requirement for moderate MAS and low-power decoupling to yield high-resolution heteronuclear spectra is the presence of large-amplitude fast motions that lead to sufficiently low order parameters, the approach should also be applicable to polypeptides that undergo fast uniaxial diffusion in lipid membranes. Several examples of such membrane protein diffusion have been reported [14,24–26]. Hydrated membrane peptide samples often contain significant levels of associated salt, thus the reduction of rf irradiation and heating by low-power decoupling is highly desirable.

We use the transmembrane domain of the influenza A M2 protein (M2TMP) to demonstrate the low-power decoupling method. The M2 protein is a proton channel important for the influenza life cycle, and is effectively blocked by the drug amantadine [27]. The 25-residue transmembrane domain forms a tetrameric helical bundle in lipid bilayers [13,28,29]. In simple phosphocholine membranes such as DLPC, DMPC and POPC at physiological temperature, the M2TMP helical bundles undergo rotational diffusion

around the bilayer normal at rates faster than the ²H quadrupolar interaction [14]. Typical C–H dipolar order parameters in M2TMP range from 0.4 to 0.6, while the variations in the N–H order parameters are larger due to their sensitivity to the helix orientation [16,30]. Fig. 7(a and b) show the ¹⁵N CP spectra of amantadine-bound M2TMP in DLPC bilayers. The spectra were acquired under 11 kHz MAS with 2 kHz WALTZ-16 decoupling and 63 kHz TPPM decoupling. The low-power decoupled spectra have 70–80% of the intensities of the high-power decoupled spectra. This is remarkable, considering that the overall oligomeric size of the protein is about 11 kDa. The rigid-limit one-bond N–H dipolar coupling is about 10 kHz, a factor of two smaller than the one-bond C–H dipolar coupling. The nearest neighbor H^N–H^α dipolar coupling is about 5.2 kHz for a distance of ~2.5 Å. Thus, if we assume a local segmental order parameter of ~0.5, the residual N-H dipolar coupling prefactor under 11 kHz MAS is estimated as:

$$\frac{\overline{\omega}_{skl}}{\omega_r} \propto \frac{(2\pi \times 10 \times 0.5 \text{ kHz}) \times (2\pi \times 5.2 \times 0.5 \text{ kHz})}{2\pi \times 11 \text{ kHz}} \approx 2\pi \times 1.2 \text{ kHz},$$

(10)

which explains why the combination of 11–13 kHz MAS and 2 kHz decoupling is adequate to give reasonable lineshape.

With 2 kHz ¹H decoupling the recycle delay is no longer limited by the rf duty cycle, thus much faster signal averaging can be car-
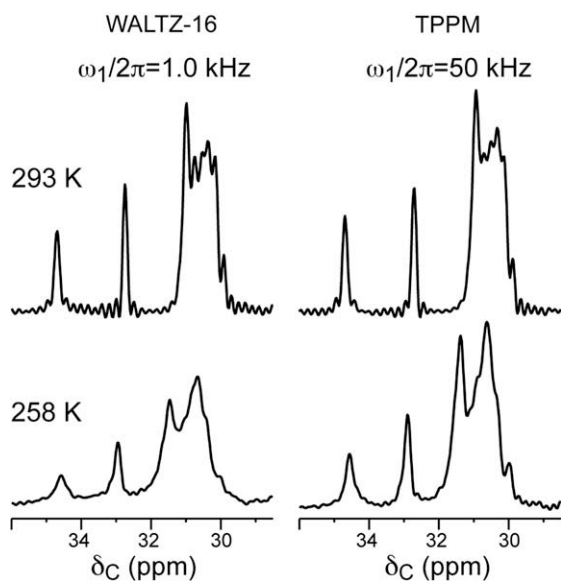
Fig. 5. ^{13}C direct-polarization spectra of hydrated POPC membranes under 11 kHz MAS as a function of temperature and ^{1}H decoupling field strength. Top spectra: 293 K. Bottom spectra: 258 K. Left column: WALTZ-16 decoupling at 1.0 kHz. Right column: TPPM decoupling at 50 kHz field strength.

ried out. Indeed, the limiting factor in the low-power decoupled CP experiments is the ^{1}H T_1, which is usually in the hundreds of milisecond range for membrane samples. Fig. 7(c and d) compares the M2TMP ^{15}N CPMAS spectrum acquired with a recycle delay of 1.0 s and 23,040 scans under 2 kHz decoupling, with a spectrum acquired under regular high-power decoupling but a recycle delay of 2.5 s and 9216 scans. The low-power decoupled spectrum gave ∼1.3 times higher intensities than the high-power decoupled spectra in the same amount of experimental time.

To obtain similarly narrow ^{13}C spectra should in principle require higher MAS rates and ^{1}H decoupling fields due to the stron-

ger C–H dipolar couplings. Yet Fig. 8 shows that the peptide ^{13}C signals with 2 kHz ^{1}H decoupling still have 70–80% of the intensities of the high-power decoupled ^{13}C spectrum. However, this comparison is limited by the fact that the M2TMP motional rates are not much faster than the C–H dipolar couplings at this temperature, so that the ^{13}C resonances are broader than ^{15}N peaks even in the high-power decoupled spectrum.

These ^{13}C and ^{15}N peptide spectra indicate that for low-power decoupling to be useful for membrane peptides, the molecular motion needs to be well into the fast regime, and slightly higher MAS frequencies is also desirable to fully recover the intensity of the high-power decoupled spectra. We predict that 3.2 mm rotors that allow spinning rates of 15–20 kHz will provide the best combination of sample volume and low-power decoupling efficiency for mobile membrane peptides.

4. Conclusion

We have shown that moderate MAS frequencies of 10–15 kHz combined with very low ^{1}H decoupling fields of 1–2 kHz are sufficient to yield high-resolution heteronuclear spectra of motionally averaged lipid membranes. The fast uniaxial diffusion removes the homonuclear dipolar coupling cross-terms in the average Hamiltonian, thus suppressing spin diffusion. For lipids with order parameters of less than 0.25, the low-power decoupled ^{13}C spectra have equal intensities compared to the high-power decoupled spectra at the same acquisition times. But by allowing much longer acquisition times to be used, low-power decoupling in practice results in significant enhancement of sensitivity and resolution. For systems with order parameters of ∼0.5, MAS frequencies of 11 kHz combined with low-power decoupling do not fully recover the high-power intensities. Nevertheless, it is possible to obtain low-power decoupled ^{15}N and ^{13}C spectra with 70–80% intensity of the high-power spectra on a membrane peptide assembly with an effective molecular weight of 11 kDa. This opens up the intriguing possibility of determining membrane peptide structures in li-
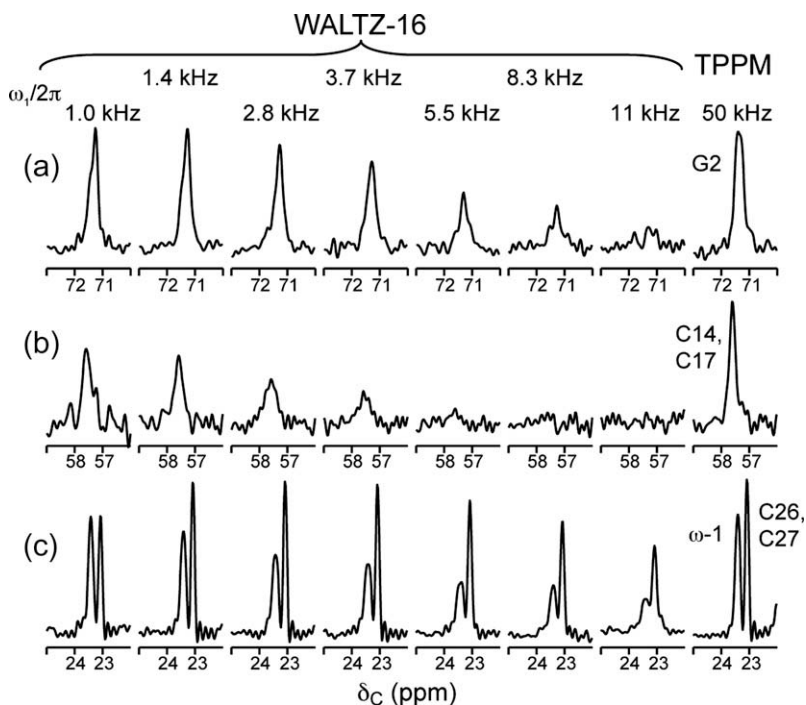

Fig. 6. Expanded regions of POPC/cholesterol spectra at 293 K under 11 kHz MAS with different ^{1}H decoupling fields. (a) POPC glycerol G2 peak. (b) Cholesterol ring C14 and C17 peaks. (c) Cholesterol aliphatic C26 and C27 peaks and the POPC $\omega - 1$ peak. The assignment of cholesterol resonances is based on reference [31].

WALTZ-16
$\omega_1/2\pi = 2.0$ kHz

TPPM
$\omega_1/2\pi = 62.5$ kHz

(a) V28, L36   S31

(b)
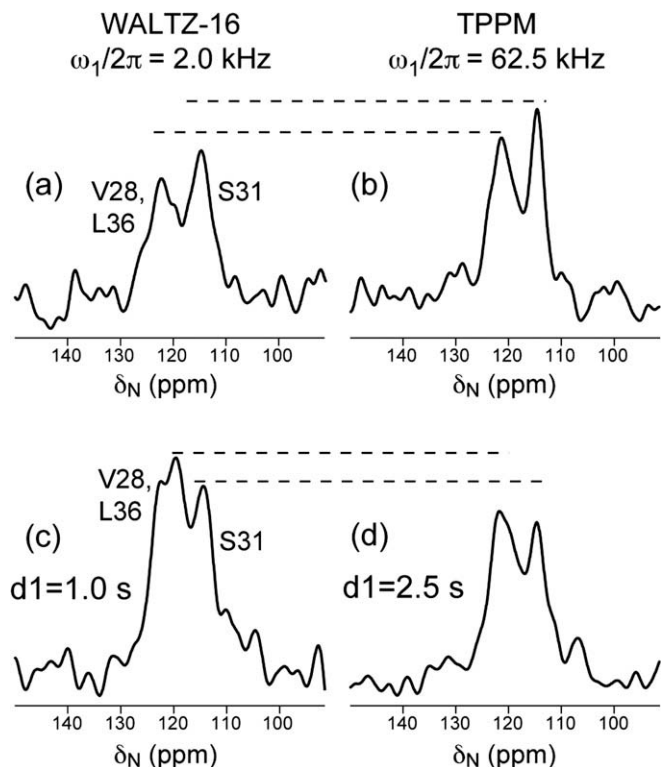
(c) V28, L36   S31   d1=1.0 s

(d) d1=2.5 s

Fig. 7. ^{15}N CP spectra of V28, S31, L36-labeled M2TMP at 313 K in DLPC bilayers under 11 kHz MAS with an acquisition time of 17.6 ms. (a) 2 kHz WALTZ-16 decoupled spectrum. (b) 63 kHz TPPM decoupled spectrum. Intensities in the low-power decoupled spectra are 70–80% of the high-power decoupled intensities. (c) 2 kHz WALTZ-16 decoupled spectrum measured with a recycle delay of 1.0 s and 23,040 scans. (d) 63 kHz TPPM decoupled spectrum measured with a 2.5 s recycle delay and 9216 scans. The fast-recycled low-power decoupled spectra have 1.3 times higher intensities than the high-power decoupled spectrum in the same total experimental time.
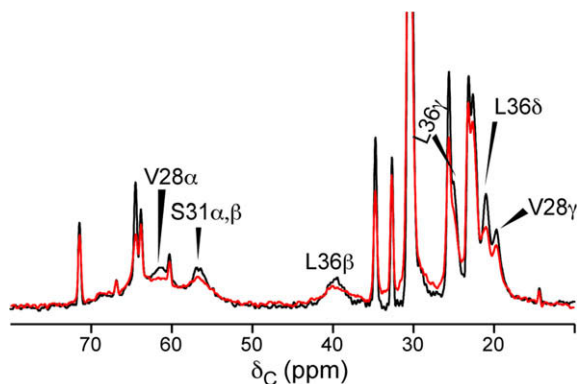

Fig. 8. ^{13}C CP spectra of V28, S31, and L36-labeled M2TMP in DLPC bilayers at 313 K under 11 kHz MAS. Black: TPPM decoupling at 63 kHz. Red: WALTZ-16 decoupling at 2 kHz. Peptide ^{13}C peaks are assigned. The low-power decoupled intensities are 70–80% those of the high-power decoupled spectra. The two spectra used the same number of scans and recycle delays. Similar to Fig. 7, if the low-power decoupled spectrum were measured with shorter recycle delays higher intensities would result in the same experimental time.

pid bilayers using liquid-state NMR spectrometers equipped with MAS probes.

Acknowledgments

References

[1] M. Ernst, A. Samoson, B. Meier, Low-power decoupling in fast magic-angle spinning NMR, Chem. Phys. Lett. 348 (2001) 293–302.
[2] M. Ernst, A. Samoson, B. Meier, Low-power XiX decoupling in MAS NMR experiments, J. Magn. Reson. 163 (2003) 332–339.
[3] M. Ernst, M. Meier, T. Tuherm, A. Samoson, B. Meier, Low-power high-resolution solid-state NMR of peptides and proteins, J. Am. Chem. Soc. 126 (2004) 4764–4765.
[4] X. Filip, C. Tripon, C. Filip, Heteronuclear decoupling under fast MAS by a rotor-synchronized Hahn-echo pulse train, J. Magn. Reson. 176 (2005) 239–243.
[5] M. Kotecha, N.P. Wickramasinghe, Y. Ishii, Efficient low-power heteronuclear decoupling in 13C high-resolution solid-state NMR under fast magic angle spinning, Magn. Reson. Chem. 45 (2007) S221–S230.
[6] T.G. Oas, R.G. Griffin, M.H. Levitt, Rotary resonance recoupling of dipolar interactions in solid-state NMR spectroscopy, J. Chem. Phys. 89 (1988) 692–695.
[7] J.A. Stringer, C.E. Bronnimann, C.G. Mullen, D.H. Zhou, S.A. Stellfox, Y. Li, E.H. Williams, C.M. Rienstra, Reduction of RF-induced sample heating with a scroll coil resonator structure for solid-state NMR probes, J. Magn. Reson. 173 (2005) 40–48.
[8] Z. Zhou, B.G. Sayer, R.E. Stark, R.M. Epand, High-resolution magic-angle spinning 1H nuclear magnetic resonance studies of lipid dispersions using spherical glass ampoules, Chem. Phys. Lipids 90 (1997) 45–53.
[9] M. Brouchard, J. Davis, M. Auger, High-speed magic angle spinning solid-state 1H nuclear magnetic resonance study of the conformation of gramicidin A in lipid bilayers, Biophys. J. 69 (1995) 1933–1938.
[10] J. Davis, M. Auger, R. Hodges, High-resolution 1H nuclear magnetic resonance of a transmembrane peptide, Biophys. J. 69 (1995) 1917–1932.
[11] O. Soubias, M. Piotto, O. Saurel, O. Assemat, V. Reat, A. Milon, Detection of natural abundance 1H–13C correlations of cholesterol in its membrane environment using a gradient enhanced HSQC experiment under high resolution magic angle spinning, J. Magn. Reson. 165 (2003) 303–308.
[12] C. Fares, F. Sharom, J. Davis, 15N, 1H heteronuclear correlation NMR of gramicidin A in DMPC-d67, J. Am. Chem. Soc. 124 (2002) 11232–11233.
[13] L.J. Holsinger, D. Nichani, L.H. Pinto, R.A. Lamb, Influenza A virus M2 ion channel protein: a structure–function analysis, J. Virol. 68 (1994) 1551–1563.
[14] S.D. Cady, C. Goodman, C. Tatko, W.F. DeGrado, M. Hong, Determining the orientation of uniaxially rotating membrane proteins using unoriented samples: a 2H, 13C, and 15N solid-state NMR investigation of the dynamics and orientation of a transmembrane helical bundle, J. Am. Chem. Soc. 129 (2007) 5719–5729.
[15] S. Cady, T. Mishanina, M. Hong, Structure of amantadine-bound M2 transmembrane peptide of influenza A in lipid bilayers from magic-angle-spinning solid-state NMR: the role of Ser31 in amantidine binding, J. Mol. Biol. 385 (2009) 1127–1141.
[16] S.D. Cady, M. Hong, Amantadine-induced conformational and dynamical changes of the influenza M2 transmembrane proton channel, Proc. Natl. Acad. Sci. USA 105 (2008) 1483–1488.
[17] A.J. Shaka, J. Keeler, T. Frenkiel, R. Freeman, An improved sequence for broadband decoupling: WALTZ-16, J. Magn. Reson. 52 (1983) 335–338.
[18] A.E. Bennett, C.M. Rienstra, M. Auger, K.V. Lakshmi, R.G. Griffin, Heteronuclear decoupling in rotating solids, J. Chem. Phys. 103 (1995) 6951–6958.
[19] M. Hong, K. Schmidt-Rohr, D. Nanz, Study of phospholipid structure by 1H, 13C, and 31P dipolar couplings from 2D NMR, Biophys. J. 69 (1995) 1939–1950.
[20] M. Hong, K. Schmidt-Rohr, A. Pines, NMR measurement of signs and magnitudes of C–H dipolar couplings in lecithin, J. Am. Chem. Soc. 117 (1995) 3310–3311.
[21] M. Ernst, A. Verhoeven, B.H. Meier, High-speed magic-angle spinning 13C MAS NMR spectra of adamantane: self-decoupling of the heteronuclear scalar interaction and proton spin diffusion, J. Magn. Reson. 130 (1998) 176–185.
[22] T.-H. Huang, C.W.B. Lee, S.K. Des Gupta, A. Blume, R.G. Griffin, A 13C and 2H nuclear magnetic resonance study of phosphatidylcholine/cholesterol interactions: characterization of liquid–gel phases, Biochemistry 32 (1993) 13277–13287.
[23] J. Urbina, S. Pekerar, H. Le, J. Patterson, B. Montez, E. Oldfield, Molecular order and dynamics of phosphatidylcholine bilayer membranes in the presence of cholesterol, ergosterol and lanosterol: a comparative study using 2H-, 13C- and 31P-NMR spectroscopy, Biochim. Biophys. Acta 1238 (1995) 163–176.
[24] M. Hong, T. Doherty, Orientation determination of membrane-disruptive proteins using powder samples and rotational diffusion: a simple solid-state NMR approach, Chem. Phys. Lett. 432 (2006) 296–300.
[25] C. Aisenbrey, B. Bechinger, Investigations of polypeptide rotational diffusion in aligned membranes by 2H and 15N solid-state NMR spectroscopy, J. Am. Chem. Soc. 126 (2004) 16676–16683.
[26] B.A. Lewis, G.S. Harbison, J. Herzfeld, R.G. Griffin, NMR structural analysis of a membrane protein: bacteriorhodopsin peptide backbone orientation and motion, Biochemistry 24 (1985) 4671–4679.
[27] L.H. Pinto, R.A. Lamb, The M2 proton channels of influenza A and B viruses, J. Biol. Chem. 281 (2006) 8997–9000.

[28] T. Sakaguchi, Q. Tu, L.H. Pinto, R.A. Lamb, The active oligomeric state of the minimalistic influenza virus M2 ion channel is a tetramer, Proc. Natl. Acad. Sci. USA 94 (1997) 5000–5005.

[29] W. Luo, M. Hong, Determination of the oligomeric number and intermolecular distances of membrane protein assemblies by anisotropic 1H-driven spin diffusion NMR spectroscopy, J. Am. Chem. Soc. 128 (2006) 7242–7251.

[30] J. Hu, T. Asbury, S. Achuthan, C. Li, R. Bertram, J.R. Quine, R. Fu, T.A. Cross, Backbone structure of the amantadine-blocked trans-membrane domain M2 proton channel from influenza A virus, Biophys. J. 92 (2007) 4335–4343.

[31] O. Soubias, F. Jolibois, V. Reat, A. Milon, Understanding sterol-membrane interactions, part II: complete 1H and 13C assignments by solid-state NMR spectroscopy and determination of the hydrogen-bonding partners of cholesterol in a lipid bilayer, Chem. Eur. J. 10 (2004) 6005–6014.